Proceedings of the 6th International Conference on Gas Hydrates (ICGH 2008), Vancouver, British Columbia, CANADA, July 6-10, 2008.

EXPERIMENTAL HYDRATE FORMATION AND GAS PRODUCTION SCENARIOS BASED ON CO_2 SEQUESTRATION.

James C. Stevens and James J. Howard*
Reservoir Laboratories, Bartlesville Technology Center
ConocoPhillips
Bartlesville, OK 74004
USA

Bernie A. Baldwin
Green Country Petrophysics LLC
Dewey, OK 74029
USA

Geir Ersland, Jarle Husebø, and Arne Graue
Department of Physics and Technology
Allegaten 55
University of Bergen
N-5007, Bergen
NORWAY

ABSTRACT

A number of laboratory experiments have investigated the rates and mechanisms of hydrate formation in coarse-grain porous media. They have shown the importance of initial water saturation and salinity on forming methane hydrates in mostly excess gas systems. Many of these experiments were conducted in a sample holder fitted within a MRI instrument that allowed for a unique method of monitoring hydrate formation by the loss of signal intensity as water and free gas are converted into a solid phase. The hydrate-saturated samples were then subjected to various procedures to release the methane. Most of the experiments focused on the exchange of carbon dioxide for methane in the hydrate. The rates and efficiency of the exchange process were reproducible over a series of initial conditions, with the notable observation that no free water was observed during the exchange process. Permeability measurements on hydrate-saturated core indicate a finite level of permeability to gas, even in cores where all of the free water was converted to hydrate.

.

Keywords: hydrate formation, CO_2 exchange, gas production

NOMENCLATURE

Sw Water saturation[fraction]

INTRODUCTION

Interest in natural gas hydrates as a potential energy resource has grown significantly in recent years as awareness of the volumes of recoverable gas becomes more focused [1]. Much of the initial efforts on planning production strategies has emphasized depressurization and/or thermal stimulation of the reservoir that in turn leads to hydrate dissociation [2]. The evaluation of potential production scenarios also requires knowledge of the recovery efficiency of the natural gas from the hydrate and the corresponding amounts of produced water. This study focuses on the exchange of CO_2 with the natural gas hydrate and the subsequent release of free CH_4.

* Corresponding author: Phone: +1.918.661.9575 E-mail: james.j.howard@conocophillips.com

Several previous experimental studies have investigated the CO_2-CH_4 exchange mechanism as a possible means of producing methane from hydrates [3,4]. These studies emphasized the thermodynamic driving forces that favor this exchange reaction, though many of the results showed significant kinetic limitations. Many of these early studies dealt with bulk methane hydrate samples placed in contact with liquid or gaseous CO_2, where available surfaces for interaction were limited. Several studies of the CO_2 exchange process in sediments showed slow methane production when the P-T conditions were near the methane hydrate stability and at CO_2 pressure values near saturation levels [5,6]. This study revisits the CO_2 exchange process in hydrates formed in porous media and takes advantage of Magnetic Resonance Imaging (MRI) technology to monitor the progress of these reactions. MRI is an especially useful method for studying hydrates in porous media since it easily detects the hydrogen in free water and methane gas, but cannot resolve hydrogen in solid phases [7,8]. The loss of signal intensity makes for a clear indicator of hydrate formation.

PROCEDURES

Hydrates were formed in the pore space of a high porosity, high permeability sandstone acquired from the Bentheim quarry in Lower Saxony, Germany. The Bentheim sample used in these experiments had a porosity of 23% and a permeability of 1100 mD and was characterized by uniform pore geometry with an average pore diameter of 125 microns. Two core plug geometries were used in these experiments. The first was a standard cylindrical plug, 3.75 cm diameter and varying lengths between 4 and 6 cm. The second arrangement split an original cylinder down the long axis of the plug and inserted a 4 mm thick acetal polyoxymethylene, POM, spacer between the two halves. The spacer had a known volume of free space and small openings in the supporting frame such that fluids could easily enter and leave the spacer. The purpose of the spacer was to simulate a fracture opening in the sample where fluids had enhanced access to the porous media. The spacer also proved to be an effective region for the accumulation of produced gas from the hydrates.

The cylindrical core-plug or plug halves plus spacer assembly was encased in shrink tubing before placement in the sleeve of the sample holder. The shrink tubing isolated the core plug from the confining fluid. The sample holder was designed for use in a Magnetic Resonance Imager, MRI, and was constructed of low-inductance fiberglass and titanium end pieces that minimized the loss of RF signal in the MRI experiments. The end pieces had multiple ports for fluids and temperature sensors. Confining pressure was applied though circulating Fluorinert™ through the sample holder. A liner composed of Aflas® prevented the loss of Fluorinert through the walls of the fiberglass housing. The Fluorinert was cooled with a bath located several meters from the sample holder and the MRI. The circulation of Fluorinert through the sample cell provided the confining pressure and maintained temperature stability within 0.1^{o}C for months at a time (Figure 1).

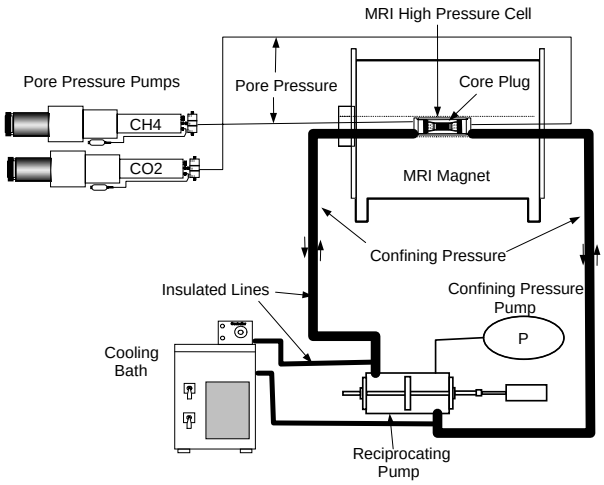

Figure 1. Schematic of hydrate experimental setup with sample cell positioned within MRI.

The introduction of fluids to the core sample was controlled by a series of pumps connected to the inlet ports on the sample holder's end pieces. Flow rates, pressures and volumes of water, nitrogen, and methane gas were controlled by these pumps.

The distribution of the initial water saturation was measured by MRI scans prior to starting the hydrate formation experiment. Sometimes the process of core assembly and water introduction was repeated several times until a uniform saturation distribution was obtained. Water salinity varied from 0.1 to 5.0 weight percent NaCl although most of the experiments were run with salinities in the range of 0.1 and 3.0 weight percent that corresponded to values anticipated in

permafrost-related hydrate deposits [1,9]. The presence of salt, which acts as a hydrate formation inhibitor, ensured that not all of the water was transformed into hydrate.

Methane gas was added to the water-saturated core plug through the inlet lines at a pore pressure of 8.3 MPa (1200 psi). The methane pressure in the system was kept constant with a Quizix pump so that any pressure reduction associated with methane consumption during hydrate formation was compensated by a measurable methane volume increase that maintained the system's constant pressure. The sequence of introducing methane and water was switched on several experiments where the pores were initially saturated with methane at a pore pressure of 8.3 MPa before the water volume was added.

The core plug assembly was cooled to 3 to 4^{o}C through the circulation of the chilled Fluorinert through the sample holder. This process generally required 2 to 6 hours to drop from room temperature to the experimental run temperature. Once at the desired temperature the sample holder was held at constant temperature, pore pressure and confining pressure for a several days period as the water and gas combined to form methane hydrate. Throughout this process the temperature, pressures and pump volumes were recorded with a standard data logging arrangement.

MRI-based data was acquired throughout the hydrate formation process with several types of images and scans. The MRI (Unity/Inova-Imaging 85/310 spectrometer, Varian Inc., Palo Alto, CA) operated at a resonance frequency of 85.7 MHz (approximately 2.0 Tesla) for hydrogen measurements. Standard 2D and 3D spin echo acquisition sequences were run with sufficient signal averaging that some of the images required up to 9 hours. The most useful information was collected as 3D images with a field of view set to 110 x 60 x 60 mm for a 128 x 32 x 32 read out and phase encoding. The resultant voxel size was 0.86 x 1.88 x 1.88 mm, which represented a sensitive volume that was comprised of several pores. The intensity in each volume therefore represented an average saturation for each cluster of hydrate-saturated pores.

Once hydrate formation was completed liquid CO_2 was injected into the spacer between core halves or at one end of a whole core plug at a constant pressure of 8.3MPa. The cooled CO_2 displaced the remaining methane in the spacer as monitored with fast MRI profiles of the spacer region. Once the methane was removed the outlet valve was shut-in and the CO_2 reservoir was set to maintain constant pressure. Further changes in CO_2 consumption were monitored by the pump volumes. Methane production in the spacer between core halves or in a spacer behind the whole core plug was detected by changes in MRI signal intensity.

Permeability was measured at several stages of the hydrate formation process in whole cores by measuring the pressure drops across the core when dry nitrogen gas was flowed at several different rates through the sample assembly. The nitrogen flow tests were very short-lived, generally less than one minute, which minimized any water absorption by the gas. MRI profiles were collected during these tests to monitor dissociation of the methane hydrate. Nitrogen does not form a hydrate at the pressure and temperature conditions used in these experiments.

RESULTS

The formation of hydrate in these sandstone samples was notable by its completeness and rapid rate in many of the experiments run in this laboratory. Hydrate formation required 24 to 80 hours to convert all of the available free water to hydrate. The MRI images provided a unique visualization of the hydrate formation process. The loss of MRI signal intensity resulted from the conversion of free water and methane, both of which are detected by the conventional pulse sequences used in MRI imaging, into hydrate. The initial image collected prior to hydrate formation showed the standard core plug partially saturated with water, S_w=0.50, and methane gas at 8.3 MPa and room temperature. The image consists of the water and gas signals from the core and gas only in the end pieces (Figure 2).

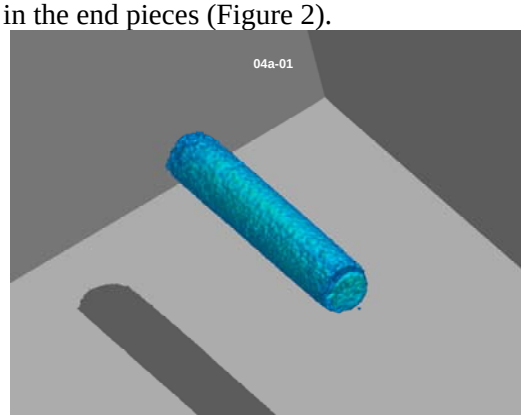

Figure 2. 3D MRI image of water saturated and methane gas-filled core plug prior to hydrate formation.

Hydrate formation began within several hours of cooling the sample to 4°C and was completed within 24 to 80 hours depending upon initial conditions of the experiment. In this experiment the only remaining signal after hydrate formation was the methane gas in the end spacers (Figure 3). The transformation of the hydrogen into a solid-state form altered the relaxation properties of the protons and made them undetectable by standard MRI pulse sequences.

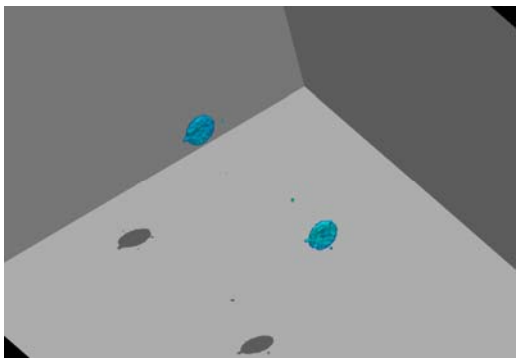

Figure 3. MRI image of whole core after hydrate formation shows complete loss of core signal. The only remaining signal resulted from free methane gas in the end pieces outside the core.

The MRI images of experiments run at higher salinity or insufficient time for total hydrate formation were characterized by small clusters of residual free water throughout the core.

The loss of MRI signal in the core during hydrate formation occurred also in the experiments with the longitudinal spacer between the core halves. The quantitative nature of the MRI-based experiments was illustrated by averaged signal intensity over the core plug region when compared to other measurements of hydrate formation. Methane consumption in the formation of hydrate matched the reduction of MRI signal of the water-saturated core sample (Figure 4). The decrease in MRI signal intensity mirrored the consumption of methane needed to form the hydrate as indicated by the increase in methane volume.

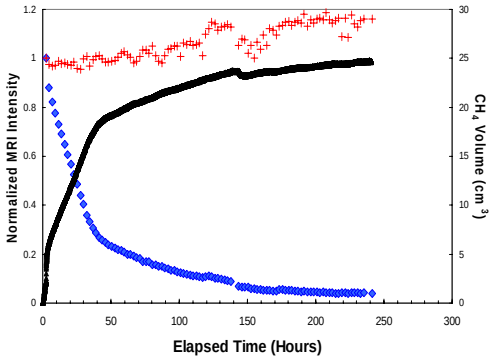

Figure 4. Methane consumption (black) compared to MRI intensity changes in the core (blue) and spacer (red) during hydrate formation.

The MRI signal of the free methane remaining in the spacer remained constant, or sometimes with a slight increase associated with small amounts of cooling of the core holder. The methane volumes were converted into molar volumes and compared directly with the MRI data. The 3D images collected during these experiments indicated that there was no specific pattern in hydrate formation, but rather it formed uniformly throughout the core in most cases.

The importance of salinity and initial water saturation on hydrate formation rates and extent were evaluated in these experiments [8,10]. Higher water salinity resulted in slower formation rates and less efficient use of the available water. Since the experiments were run with “infinite” methane gas reservoir, it was possible for most of the available free water to transform into hydrate. Remaining free water in several of the high salinity tests was generally localized in small clusters of pores that filled individual voxels in the MRI image.

The experiments with the longitudinal spacer between the core halves more clearly illustrated the methane production rates and extents after CO_2 was introduced. MRI images provided an effective means of ensuring that excess methane was displaced from the spacer by CO_2 injection (Figure 5).

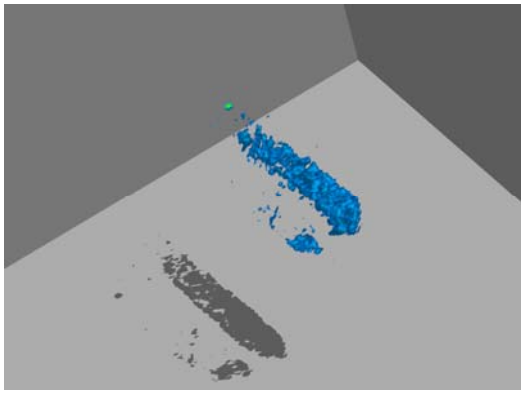

Figure 5. MRI image of core after hydrate formation and displacement of methane in spacer with CO_2. Observed signal resulted from residual water in core.

The signal in this 3D image resulted from contributions of the water in the core halves that was not converted to hydrate. The spacer between the core halves had no signal after CO_2 flushed the methane.

After the CO_2 was shut-in the spacer, a series of 3D images were collected over a several week period. MRI intensity in the spacer increased with time while the remaining signal in the core halves decreased slightly (Figure 6).

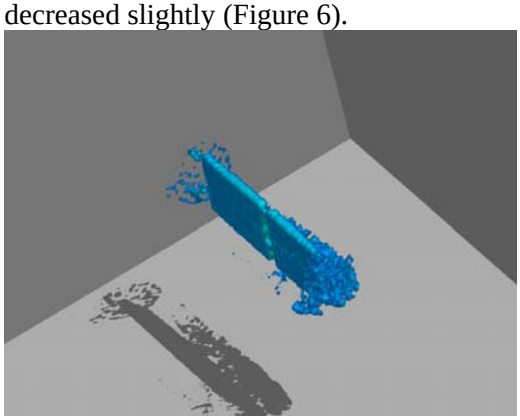

Figure 6. MRI image of spacer after methane diffused from core during exchange with CO_2.

Methane from the hydrate in the core diffused into the spacer during this time. The MRI intensity corresponded to methane molar volumes that far exceeded any free methane that might have remained in the pores after hydrate formation. Mass balance calculations indicated that most, if not all, of the methane that accumulated in the spacer had to come from the hydrate. The absence of any significant MRI signal in the core during this time suggested that no large-scale dissociation took place that released significant volumes of free water. Instead, the decrease in MRI signal in the core indicated that any remaining free water after methane hydrate formation was converted into a CO_2 hydrate.

As before, the MRI images provided quantitative data that was compared with other indicators of hydrate formation and exchange. One advantage of the MRI data was the spatial information it contained. In addition to average signal changes that were determined for the entire core, it was possible to focus on changes restricted to certain portions of the core or spacer [11]. The loss of signal MRI intensity in the core was countered by the increased methane volume consumed during hydrate formation as noted above.

The MRI intensity remained constant in the spacer during hydrate formation until CO_2 was flushed through the spacer at 180 hours and the intensity dropped to zero (Figure 7). The methane volume after 150 hours was an artifact of closing the line to the sample cell; the data recorder continued to detect a constant, if meaningless, value.

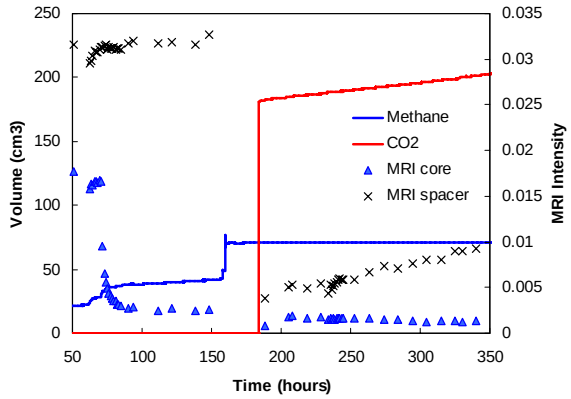

Figure 7. MRI average signal intensity for core and spacer compared to methane and CO_2 pump volumes collected during hydrate formation and exchange with CO_2.

It was noted that in all of the experiments run in this system that the MRI images did not detect any significant increase in signal in the hydrate-saturated cores that would indicate the presence of free water during CO_2 exchange. This was verified by the evaluation of the MRI signal intensity in the core halves once CO_2 exchange began after 180 hours. MRI intensity remained constant and even was less than the baseline value after the completion of methane hydrate formation. The

implication was that the exchange process did not cause significant dissociation of the hydrate, at least on the scale of the MRI's spatial resolution of ~0.8 mm^3. These experiments were run at CO_2 partial pressures significantly greater than CO_2 saturation levels, in contrast to earlier studies where the CO_2 levels were only slightly in excess to saturation or were undersaturated [5,6].

The exchange of CO_2 for methane in the hydrate structure was monitored by the consumption of CO_2 volumes and by the increase in the MRI signal intensity in the spacer region (Figure 8).

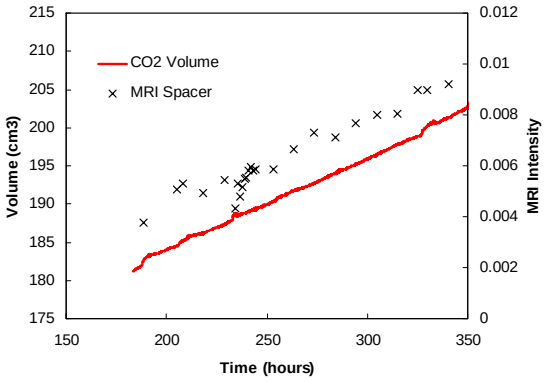

Figure 8. MRI intensity of spacer region during production of methane from hydrate in core compared to the consumption of CO_2.

A comparison of the CO_2 pump log and the MRI images showed that the production of methane into the spacer as monitored by MRI intensity was closely mirrored by the consumption of CO_2. It was also noteworthy that methane release from the hydrate occurred at temperature and pressures significantly greater than the methane-hydrate stability region, suggesting that the driving forces for CO_2 hydrate formation were significantly large and the associated absence of any free water to reform methane hydrate.

Partially water-saturated core plugs prior to hydrate formation had permeability values in the range of several hundred millidarcies. These experiments were run with initial water saturations of 0.34 and 0.51. In both cases hydrate formation continued until virtually all of the free water was converted into hydrate. As the samples were cooled to 4°C and hydrate formation began these permeabilities were monitored at several stages during formation. After hydrate formation ceased the permeability ranged between 1 to 25 mD (Figure 9).

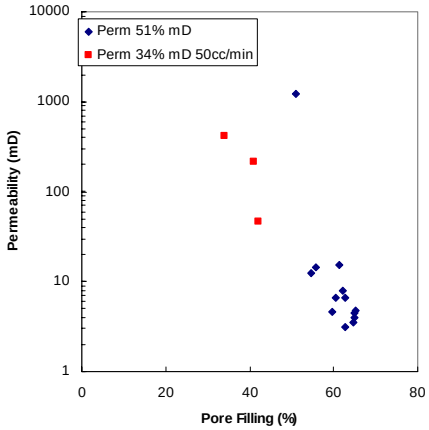

Figure 9. Permeability of hydrate-saturated samples as function of percentage of pore volume filled with hydrate and free water.

The pore filling parameter represents the sum of remaining free water and hydrate in the pore space and was determined from the combination of the initial water saturation, the conversion of water to hydrate as determined by MRI measurements and a constant expansion term for the hydrate relative to water. The combination of two experiments with different initial water saturations that led to a range of pore filling values suggested a common trend of permeability decrease for this particular pore geometry.

CONCLUSIONS

The laboratory setup was used successfully to form methane hydrate in sandstone pores under a range of initial water saturation, salinity and temperature-pressure conditions. The MRI capability of the setup provided an additional method to monitor hydrate formation along with conventional gas consumption logs. Experiments run with excess methane and low water salinity generally resulted in all of the free water

transforming into hydrate. Higher water salinity resulted in slower formation rates and incomplete transformation of the water into hydrate.

The introduction of CO_2 into the longitudinal spacer in the main core design provided a means to follow the formation of CO_2-hydrate at the expense of the initial methane hydrate. Diffusion processes appeared to be the dominant driving mechanism in supplying CO_2 to the methane hydrate reaction sites and the concomitant increase of methane in the spacer. The exchange process was rapid and efficient in that no free water was observed in the core with MRI measurements. The spatial resolution of the MRI measurement does not rule out the possibility of small-scale dissociation and reformation of the hydrate phases, and in truth the creation of a thin-water film helps explain the rapid reaction rates [12]. Injection of CO_2 into the whole-core hydrate-saturated pore system resulted in methane production at the outlet end.

Permeability measured in these core plugs during hydrate formation decreased to low values, but at levels sufficient for gas transport. These reduced permeability values remained constant during the CH_4-CO_2 exchange process in the hydrate structure.

REFERENCES

[1] Sloan ED, Koh, C. *Clathrate hydrates of natural gases*, 3rd ed. Boca Raton: CRC Press, 2008.

[2] Moridis G, Kowalsky M, Pruess K. *Depressurization-induced gas production from class-1 hydrate deposits*. SPE Reservoir Eval. & Eng. 2007; 10(5):458-481.

[3] Ohgaki K, Takano K, Sangawa H, Matsubara T, Nakano S. *Methane exploitation by carbon dioxide from gas hydrates – phase equilibria for CO_2-CH_4 mixed hydrate system*. J. Chem. Eng. Jpn. 1996; 29(3): 478-483.

[4] Hirohama S, Shimoyama Y, Tatsuta S, Nishida N. *Conversion of CH_4 hydrate to CO_2 hydrate in liquid CO_2*. J. Chem. Eng. Jpn. 1996; 29(6): 1014-1020.

[5] Jadhawar P, Yang J, Jadhawar J, Tohidi B. *Preliminary experimental investigation on replacing methane in hydrate structure with carbon dioxide in porous media. In: Proceedings of the Fifth International Conference on Gas Hydates*, 2005.

[6] Sivaraman R. *The potential role of hydrate technology in sequestering carbon dioxide*. Gas Tips News Letter; 2003, Gas Technology Inst.

[7] Kleinberg R. *Nuclear magnetic resonance pore scale investigation of permafrost and gas hydrate sediments*. In: Rothwell G, editor. New Methods of Core Analysis: Principles and Applications. London: Geol. Soc, 2005.

[8] Stevens J, Baldwin B, Graue A, Ersland G, Husebø J, Howard J. *Measurements of hydrate formation in sandstone*. Petrophysics, 2008; 49(1): 67-73.

[9] Makogan Y. *Hydrates of hydrocarbons*. Tulsa, Pennwell Books, 1997.

[10] Ersland G, Husebø J, Graue A, Baldwin B, Howard J, Stevens J, Zornes D. *Measuring gas hydrate-CO_2 exchange in Bentheim sandstone using MRI tomography and IDL-programming. In: 5th World Congress on Industrial Process Tomography*, 2007.

[11] Husebø J, Ersland G, Stevens J, Kvamme B, Graue A. *The effect of brine salinity on fill fraction and formation pattern of methane hydrates in sandstone: In: Proceedings of the Sixth International Conference on Gas Hydates*, 2008.

[12] Graue A, Kvamme B, Baldwin B, Stevens J, Howard J, Aspenes E, Ersland G, Husebø J, Zornes D. *Environmentally friendly CO_2 storage in hydrate reservoirs benefits from associated spontaneous methane production. In: Offshore Technology Conference Proceedings, Paper 18087*, 2006.